Parametric polariton solitons in coherently pumped semiconductor microcavities

O. A. Egorov,[1,*] D. V. Skryabin,[2] and F. Lederer[1]

[1]*Institute of Condensed Matter Theory and Solid State Optics, Abbe Center of Photonics, Friedrich-Schiller-Universität Jena, Max-Wien-Platz 1, D-07743 Jena, Germany*

[2]*Centre for Photonics and Photonic Materials, Department of Physics, University of Bath, Bath BA2 7AY, United Kingdom*

(Received 6 July 2011; published 4 October 2011)

We demonstrate the existence of parametric solitons due to four-wave mixing in a coherently pumped semiconductor microcavity operating in the strong-coupling regime. These spatial solitons are localized in the direction perpendicular to the pump momentum and form periodic trains of pulses in the direction parallel to it. The parametric solitons constitute a family continuously parameterized by the energies and momenta of the signal and idler components. They also play a profound role in the formation of two-dimensional polariton solitons.

DOI: 10.1103/PhysRevB.84.165305 PACS number(s): 42.65.Pc, 71.36.+c, 42.65.Tg, 42.65.Sf

I. INTRODUCTION

Currently, there is a growing body of research on collective nonlinear dynamics of half-light/half-matter quasiparticles (polaritons) being formed as a result of strong light-matter interaction. One prominent example of such polaritons is exciton polaritons in semiconductor microresonators operating in the strong-coupling regime,[1–5] which exhibit a strong and fast excitonic nonlinearity.[4–7] This nonlinearity is by far faster and stronger than the relevant photonic nonlinearity in resonators in the weak-coupling regime. In the past few years extensive studies of microcavity polaritons have been largely motivated by the investigation of Bose-Einstein condensation[8–10] and superfluidity.[10–14] Depending on the semiconductor material used, exciton polaritons have been observed at temperatures reaching from a few kelvins[1] to room temperature.[2,15] The latter has further boosted their potential for practical applications.

The strong repulsive interaction of excitons has been shown to lead to low-threshold optical bistability[16–18] and parametric four-wave mixing.[19–25] In particular, parametric gain can be achieved provided that the pump momentum exceeds a critical value associated with the so-called "magic angle" marking the point where the effective polariton mass changes its sign.[24] Indeed, due to the nonparabolic shape of the energy-momentum characteristic of the lower-branch polaritons, the resonant scattering of two pump polaritons into the signal-idler pair can simultaneously conserve the frequency $2\Omega(k_p) = \Omega(k_s) + \Omega(k_i)$ and kinetic momentum $2k_p = k_s + k_i$. This degenerated parametric four-wave mixing process results in the transformation of an unstable homogeneous state into a traveling roll pattern, with one of the roll's side-bands peaking close to zero momentum.[19–25]

Our recent work has demonstrated the existence of moving one-dimensional (1D) and two-dimensional (2D) localized self-trapped polaritons: *polariton solitons*.[26–28] In sharp contrast to many other solitonic systems, bright 2D polariton solitons exist for a negative effective mass along the direction of the pump momentum and a positive mass along the orthogonal direction.[28] The negative component of the diagonal mass tensor easily explains the formation of 1D bright polariton solitons, since the polariton-polariton interaction is repulsive.[26,27] However, this mechanism cannot explain the localization along the direction associated with the positive mass. The presence of the parametric four-wave mixing plays a key role here. The nonlinearity describing parametric wave mixing is not simply proportional to the wave intensity (or particle density), but involves the phases of the participating waves and thus an energy exchange between the different constituents. The nonlinearity is no longer simply attractive or repulsive and leads to solitons with novel properties in both conservative[29] and dissipative configurations (see, e.g., Refs. 30–33, and references therein).

Note that only weakly localized states, known as nonlinear *X* waves, have been found in conservative optical systems with opposite signs of temporal and spatial dispersions.[34] Unlike conservative *X* waves, 2D polariton solitons are finite-energy localized states and possess exponentially decaying tails caused by dissipation, which is associated with the picosecond lifetimes of the intracavity photons and excitons. In this paper we demonstrate that the coupled equations for the signal, idler, and pump polaritons have polariton soliton solutions localized in the direction orthogonal to the pump momentum.

In Sec. II we describe the mathematical model of a semiconductor microcavity operating in the strong coupling regime [Fig. 1(a)] and reduce it to the pertinent coupled equations. Then, in Sec. III, we prove the existence and study the properties of parametric polariton solitons. In Sec. IV we report a numerical analysis of the dynamics of parametric solitons in two dimensions, where they form trains of moving pulses. In a narrow range of parameters one pulse of this moving pattern can be excited separately, thereby forming a stable moving 2D polariton soliton.[28]

II. MATHEMATICAL MODEL

The coupled dynamics of the amplitudes of the photonic E and excitonic Ψ fields linearly polarized in the microcavity plane (TE polarization) is governed by the dimensionless system[5,26]

$$\begin{aligned} \partial_t E - i\left(\partial_x^2 + \partial_y^2\right)E + (\gamma_{\rm ph} - i\Omega_p)E &= i\Psi + E_p e^{ik_p x}, \\ \partial_t \Psi + (\gamma_{\rm ex} - i\Omega_p)\Psi + i|\Psi|^2\Psi &= iE, \end{aligned} \tag{1}$$

where E_p and k_p are the amplitude and momentum of the external pump beam and $\Omega_p = (\omega - \omega_{\rm ph})/\Omega_R$ is the detuning

of the pump frequency ω from the identical exciton and cavity resonances $\omega_{\rm ph} = \omega_{\rm ex}$ (normalized to the Rabi splitting Ω_R). $\gamma_{\rm ph}$ and $\gamma_{\rm ex}$ are the cavity and the exciton damping rates. To keep the analysis simple we assume $\gamma_{\rm ph} = \gamma_{\rm ex} = \gamma$. A unit of t corresponds to $\simeq$0.25 ps and a unit of x to $\simeq 1\ \mu$m if typical parameters of cavity polariton experiments with a single InGaAs/GaAs quantum well are used. Full details of the rescaling into physical units can be found elsewhere.[26,35]

First, we briefly discuss the linear polariton dispersion, which is defined as the dependence of the frequency Ω (or energy) from the components of the in-plane momentum k_x and k_y. Assuming that $E,\Psi \sim e^{-\gamma t}e^{-i\Omega t+ik_x x+ik_y y}$ and dropping the pump and nonlinear terms, we find the eigenvalue problem,

$$\Omega(k_x,k_y)\vec{p}_{k_x,k_y} = \begin{pmatrix} k_x^2+k_y^2 & -1 \\ -1 & 0 \end{pmatrix}\vec{p}_{k_x,k_y}, \qquad (2)$$

where $\vec{p}_{k_x,k_y} = \{e_{k_x,k_y},\psi_{k_x,k_y}\}$ is the polariton basis vector and $\Omega_\pm(k_x,k_y)$ are the eigenfrequencies. e_{k_x,k_y} and ψ_{k_x,k_y} are the amplitudes of the photonic and excitonic components (known as the Hopfield coefficients),[36] respectively. A solution of the eigenvalue problem, (2), yields the linear polariton dispersion relation

$$\Omega_\pm(k_x,k_y) = \frac{k_x^2+k_y^2}{2} \pm \sqrt{1+\frac{1}{4}\left(k_x^2+k_y^2\right)^2}, \qquad (3)$$

where $\Omega_\pm(k_x,k_y)$ are the relative frequencies of the upper (UP) and lower (LP) polariton branches, respectively (see, e.g., Ref. 5). The UP branch ($\Omega > 1$) is irrelevant for our present study, which exclusively focuses on LP branches ($-1 < \Omega < 0$) [Fig. 1(b)]. The curvature of the $\Omega(k_x,k_y)$ surface determines the second-order dispersion and thus the effective polariton mass $M_{x,y} = \frac{\hbar\omega n^2}{c^2}\left(\frac{\partial^2\Omega}{\partial k_{x,y}^2}\right)^{-1}$, where M_x and M_y denote the effective masses parallel and orthogonal to the direction of the pump momentum, respectively. c is the light velocity in vacuum and n is the averaged refractive index of the microcavity. Fixing $k_y = 0$ (as for the pump field), one finds that the effective mass M_x is positive for $k_x < k_d$ and negative for $k_x > k_d$ ($k_d \sim 0.885$).

The repulsive nonlinearity of excitons is known to give rise to bistability.[16–18] We have previously demonstrated that inside the bistability range, 1D polariton solitons exist which are localized in the direction along the pump momentum and are nested on the lower branch of the bistability loop. These solitons move with a fixed velocity determined by the pump momentum $k_p > k_d$, so that the dispersion of the negative-mass particles can be compensated by the repulsive interparticle interactions.[26] However, this mechanism cannot explain the existence of 2D bright polariton solitons exhibiting a positive effective mass along the direction orthogonal to the pump momentum, which cannot be counterbalanced by a repulsive nonlinear interaction.[35] In Ref. 28 we discussed two complimentary physical interpretations of the polariton localization along the positive-mass direction. The first one is the interaction of propagating fronts near the Maxwell point, where the velocity of the fronts is close to 0 and they are pinned, and the second, elaborated in more detail in this work, is that parametric four-wave mixing is associated with phase-dependent nonlinearity [see Eqs. (5)–(7)], which exerts complex interplay with the dispersive terms and is able to counterbalance them in the cases of both positive and negative masses.[29]

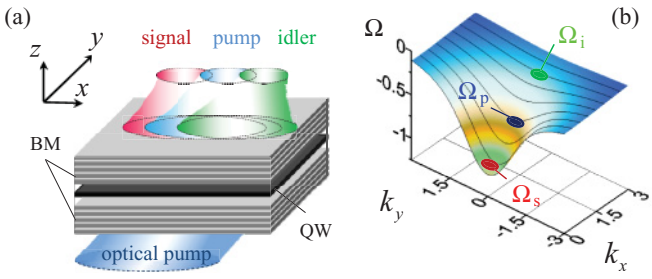

FIG. 1. (Color online) (a) Sketch of the microcavity driven by a coherent optical pump. The semiconductor quantum well (QW) is sandwiched between two Bragg mirrors (BM). (b) Dispersion of the lower polaritons (LP). Ω_p, Ω_s, and Ω_i are the frequencies of the pump, signal, and idler polaritons, respectively.

To understand the physics behind the parametric polariton soliton formation and to identify domains of their existence, we proceed by assuming that the polariton wavepacket has three components, with momenta centered around the pump ($k_x = k_p$, $k_y = 0$), signal ($k_x = k_s$, $k_y = 0$), and idler ($k_x = k_i$, $k_y = 0$) momenta, respectively. The corresponding frequencies are $\Omega_{\rm p}$, $\Omega_{\rm s}$, and $\Omega_{\rm i}$. Thus we express E and Ψ in Eqs. (1) as (see Refs. 22 and 25):

$$\begin{aligned} E(x,y,t) = {} & A_p(y,t)(e_p/\psi_p)e^{ik_p x} \\ & + A_s(y,t)(e_s/\psi_s)e^{ik_s x - i(\Omega_s-\Omega_p)t+i\delta t} \\ & + A_i(y,t)(e_i/\psi_i)e^{ik_i x - i(\Omega_i-\Omega_p)t-i\delta t}, \\ \Psi(x,y,t) = {} & A_p(y,t)e^{ik_p x} + A_s(y,t)e^{ik_s x - i(\Omega_s-\Omega_p)t+i\delta t} \\ & + A_i(y,t)e^{ik_i x - i(\Omega_i-\Omega_p)t-i\delta t}. \end{aligned} \qquad (4)$$

Here $A_{\rm p,s,i}(y,t)$ are the slowly varying complex amplitudes. $e_{\rm p,s,i}$ and $\psi_{\rm p,s,i}$ are the components of $\vec{p}_{k_x,k_y}$ [see Eq. (2)]. δ is the additional frequency shift between signal and idler polaritons. δ is a free parameter, which has to be determined self-consistently with the soliton profiles. A similar frequency shift has been used in the theory of parametric solitons in cavities with a quadratic nonlinearity.[31] Inserting ansatz (4) into Eq. (1) we derive the set of differential equations

$$\begin{aligned} & i\frac{\partial A_p}{\partial t} + D_p\frac{\partial^2 A_p}{\partial y^2} + (i\gamma+\Delta_p)A_p \\ & -\xi_p(|A_p|^2+2|A_s|^2+2|A_i|^2)A_p - 2\xi_p A_s A_i A_p^* = W, \end{aligned} \qquad (5)$$

$$\begin{aligned} & i\frac{\partial A_s}{\partial t} + D_s\frac{\partial^2 A_s}{\partial y^2} + (i\gamma+\Delta_s-\delta)A_s \\ & -\xi_s(2|A_p|^2+|A_s|^2+2|A_i|^2)A_s - \xi_s A_p^2 A_i^* = 0, \end{aligned} \qquad (6)$$

$$\begin{aligned} & i\frac{\partial A_i}{\partial t} + D_i\frac{\partial^2 A_i}{\partial y^2} + (i\gamma+\Delta_i+\delta)A_i - \\ & -\xi_i(2|A_p|^2+2|A_s|^2+|A_i|^2)A_i - \xi_i A_p^2 A_s^* = 0 \end{aligned} \qquad (7)$$

where $\Delta_{\rm p,s,i} = \Omega_{\rm p,s,i} - \Omega_-(k_{\rm p,s,i},k_y=0)$ are the effective frequency detunings of the polaritons from the frequency of

the noniteracting polaritons. The external pump amplitude is $W = \eta E_p$, where $\eta = e_p\psi_p/(|e_p|^2 + |\psi_p|^2)$. The coefficients $D_{\mathrm{p,s,i}} = \frac{\hbar\omega n^2}{c^2} M^{-1}_{p,s,i}$, where $M_{p,s,i} \equiv M_y(k_{p,s,i})$ are the y components of the effective masses of the pump, signal, and idler polaritons (Fig. 1). $\xi_{\mathrm{p,s,i}} = |\psi_{\mathrm{p,s,i}}|^2/(|e_{\mathrm{p,s,i}}|^2 + |\psi_{\mathrm{p,s,i}}|^2)$ are the coefficients describing self- and cross-interactions of the participating polaritons. Using the solution of the eigenvalue problem (2) for the coefficients $|e_{\mathrm{p,s,i}}|$ and $|\psi_{\mathrm{p,s,i}}|$, one obtains

$$\xi_{\mathrm{p,s,i}} = \frac{\left(k^2_{\mathrm{p,s,i}} + \sqrt{4 + k^4_{\mathrm{p,s,i}}}\right)^2}{\left(k^2_{\mathrm{p,s,i}} + \sqrt{4 + k^4_{\mathrm{p,s,i}}}\right)^2 + 4}. \tag{8}$$

Obviously, the transverse momentum has only a minor quantitative effect on the effective nonlinear coefficient, which increases monotonically from $\xi = 1/2$ (for $k_x = 0$) to $\xi = 1$ (for $k_x = \infty$). Thus, for convenience we may assume $\xi_{\mathrm{p,s,i}} = \xi = 1$, which does not impose any constraints on the results discussed below.

III. ONE-DIMENSIONAL PARAMETRIC POLARITON SOLITONS

Without signal and idler components ($A_{s,i} = 0$), only dark polariton solitons are stable for the repulsive (defocusing) nonlinearity and a positive polariton mass (dispersion).[35] Unstable bright solitons (BSs) bifurcate from the homogeneous solution (HS) at the point where modulational instability sets in [see the dotted line in Fig. 2(a) and the profile in Fig. 2(b)]. The BS branch terminates at the so-called Maxwell point, while touching the upper state of the HS bistability loop. Various termination scenarios of the dissipative localized structures has been the subject of intense recent research (see, e.g., Ref. 37 and references therein).

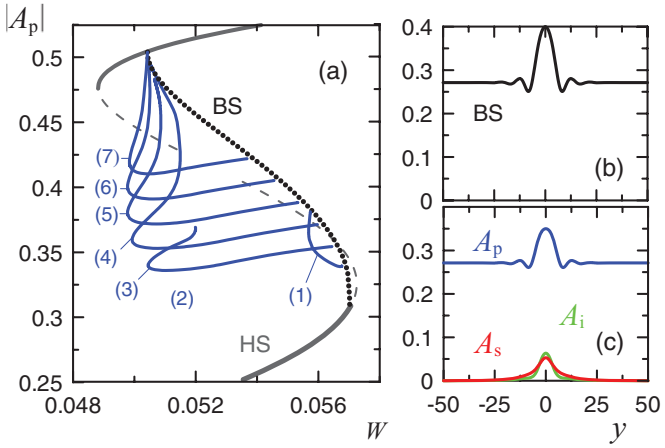

FIG. 2. (Color online) (a) Maxima of the pump component of parametric polariton solitons for different detunings of the signal component: (1) $\Delta_s = 0.15$, (2) $\Delta_s = 0.25$, (3) $\Delta_s = 0.35$, (4) $\Delta_s = 0.45$, (5) $\Delta_s = 0.55$, (6) $\Delta_s = 0.65$, and (7) $\Delta_s = 0.75$. The dotted (black) line marks the unstable pump-only bright soliton (BS), which bifurcates from the pump-only homogeneous solutions (HS). (b) Amplitude profile of the unstable pump-only BS. (c) Pump, signal, and idler components of the parametric polariton soliton close to the bifurcation point. Other parameters: $\Delta_{p,i} = 0.25$, $D_p = 0.23$, $D_s = 0.5$, and $D_i = 0.03$.

Four-wave mixing qualitatively alters the physics of polariton solitons. In the simplest case of the HS, the trivial pump-only ($A_{s,i} = 0$) solution becomes unstable, giving rise to the generation of signal and idler polaritons provided that the pump amplitude (A_p) exceeds a threshold value.[25] First, we briefly discuss the parametric threshold for the generation of small signal and idler polaritons in the undepleted pump limit ($|A_p| \gg |A_{s,i}|$). Looking for the solution of Eqs. (6) and (7) in the form $A_{s,i}(t) = a_{s,i}e^{\lambda t}$ and $A^*_{s,i}(t) = b_{s,i}e^{\lambda t}$ for the constant pump component A_p and keeping only linear terms in the fluctuations $a_{s,i}$ and $b_{s,i}$, one gets the eigenvalue problem for λ:

$$\mathrm{Re}\lambda = -\gamma \pm \sqrt{\xi^2|A_p|^4 - \tfrac{1}{4}((\Delta_s + \Delta_i) - 4\xi|A_p|^2)^2}. \tag{9}$$

The pump-only solution becomes parametrically unstable provided that the real part of the eigenvalue is positive, $\mathrm{Re}\lambda > 0$. Thus the parametric threshold can be defined as $\mathrm{Re}\lambda(|A_p|) = 0$, where the parametric instability of the trivial signal and idler states just sets in. This threshold is then given by

$$|A_{\mathrm{PT}}|^2 = \frac{2(\Delta_s + \Delta_i) \pm \sqrt{(\Delta_s + \Delta_i)^2 - 12\gamma^2}}{6\xi}. \tag{10}$$

The physics does not change qualitatively for the nonuniform pump profile. For instance, if the pump component $A_p(y)$ coincides with the pump-only BS solution [see Fig. 2(b)], the inhomogeneous signal and idler components are generated provided that the maximum of the BS amplitude exceeds the parametric threshold A_{PT} given approximately by Eq. (10) [see Fig. 2(c)].

To rigourously calculate the profile of the parametric polariton solitons beyond the nondepleting pump approximation, we used the stationary version ($\partial A_{p,s,i}/\partial t = 0$) of Eqs. (5)–(7). Note that the unknown frequency shift δ between signal and idler waves has to be calculated self-consistently with the parametric polariton soliton profile, which includes all three components. Figure 2(a) shows the parametric soliton branches for several values of the signal polariton detuning Δ_s. Both the existence domain and the shape of the parametric soliton depend strongly on this detuning. The parametric polariton soliton branches approach the pump-only BS solution close to the parametric threshold points ($|A_{\mathrm{PT}}|$). In accordance with Eq. (10) these bifurcation points shift upward along the pump-only solution branch with increasing frequency detunings of the signal and idler polaritons. More precisely, the parametric threshold is located slightly below the bifurcation point of the parametrical polariton soliton [see PPS branch and PT point in Fig. 3(a)]. A phase shift due to diffraction of the nonuniform pump component explains this small discrepancy.

The signal and idler components of the parametric polariton soliton increase away from the bifurcation point [Fig. 3(a)]. The selection rule for the frequency detuning δ between the signal and the idler components of the parametric polariton soliton is closely related to the relative energy balance. Indeed, similarly to the case of nondegenerated optical parametric oscillators (OPOs),[31] any steady-state solution, such as the

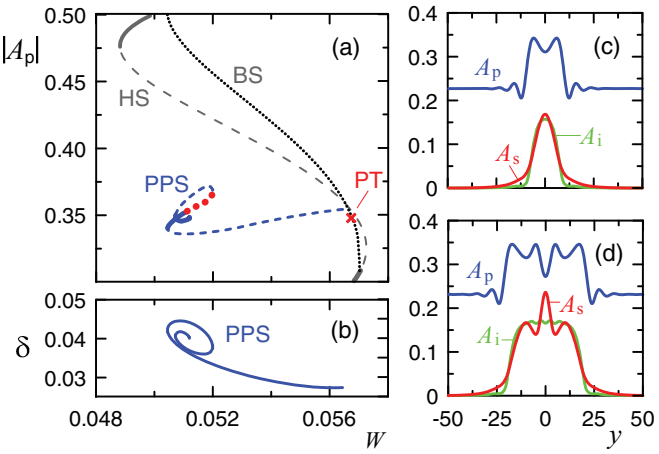

FIG. 3. (Color online) (a) Branches of homogeneous solution (HS), unstable bright soliton (BS), and parametric polariton soliton (PPS). Dashed lines represent unstable solutions. The thick dotted line shows the slightly unstable PPS (see text). PT represents the parametric threshold point given by Eq. (10). (b) Frequency shift (δ) between signal and idler components of the parametric polariton soliton vs the external pump amplitude. Amplitude profiles of (c) stable fundamental PPS for $W = 0.0505$ and (d) stable second-order PPS for $W = 0.051$. Other parameters: $\Delta_{p,i} = 0.25$, $\Delta_s = 0.35$.

soliton solutions of the model, (5)–(7), has to satisfy the condition

$$\gamma_s \int |A_s(y)|^2 dy = \gamma_i \int |A_i(y)|^2 dy, \qquad (11)$$

where $\gamma_{s,i}$ are the losses of the signal and idler polaritons (in our case, $\gamma_{s,i} = \gamma$). This additional condition for the energy balance selects a strictly defined value of the free parameter δ which can be calculated self-consistently with the soliton profile [see Fig. 3(b)]. After the turning point the soliton consists of three components comparable in their amplitudes [Figs. 3(c) and 3(d)].

It is well known that the turning points of the soliton branches are associated with saddle-node bifurcations and therefore with a change of the soliton stability (see, e.g., Refs. 30, 32, and 33). To study the stability of parametric solitons, the response of the system to a weak perturbation has to be calculated using linear stability analysis.[11] Toward this aim, we looked for the solution of Eqs. (5)–(7) around the stationary state $S_{p,s,i}(y)$ (with the corresponding value of the frequency shift δ) in the form $A_{p,s,i}(y,t) = S_{p,s,i}(y) + a_{p,s,i}(y)e^{\lambda t}$ and $A^*_{p,s,i}(y) = S^*_{p,s,i}(y,t) + b_{p,s,i}(y)e^{\lambda t}$, and keeping only linear terms in the fluctuations $a_{p,s,i}(y)$ and $b_{p,s,i}(y)$, one gets the eigenvalue problem for λ. A stationary solution $S_{p,s,i}(y)$ is stable provided that all eigenvalues of the linear perturbation spectra have negative real parts.

Figures 3(c) and 3(d) show examples of stable fundamental and second-order parametric polariton solitons. Apparently, sufficiently strong signal and idler components may stabilize the initially unstable pump-only BS. Direct numerical simulations confirm that these stable localized solutions are attractors. Therefore, they can be excited from a fairly wide range of initial conditions. It is typical for a dissipative system[38] that the system parameters determine completely the shape and the free frequency detuning δ of the parametric polariton soliton of the model, (5)–(7).

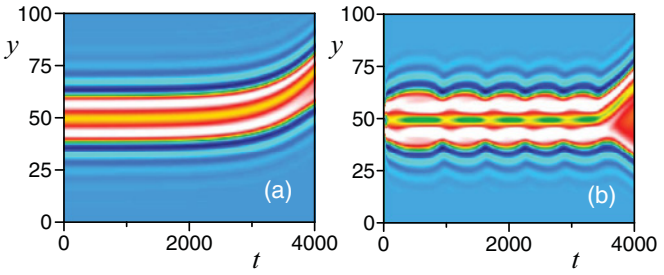

FIG. 4. (Color online) Evolution dynamics of an unstable PPS. (a) Destabilization due to an asymmetric eigenmode with $\lambda = 0.0018$ for the pump amplitude $W = 0.0511$. (b) Destabilization due to an symmetric eigenmode with $\lambda = 0.00014 \pm i0.015$ for the pump amplitude $W = 0.0517$ (b). Parameters: $\Delta_{p,i} = 0.25$, $\Delta_s = 0.35$.

Fundamental parametric polariton solitons can undergo destabilization [see thick dotted line in Fig. 3(a)]. One may anticipate two typical scenarios of their destabilization. In the first case, close to the destabilization point the linear spectrum of perturbations has an asymmetric (with respect to the soliton center y_0) eigenmode [$a_{p,s,i}(y - y_0) = -a_{p,s,i}(y_0 - y)$, $b_{p,s,i}(y - y_0) = -b_{p,s,i}(y_0 - y)$] with a purely real negative eigenvalue λ. The evolution of this eigenmode leads to spontaneous symmetry breaking of the parametric soliton profile, resulting in a transverse (y-direction) motion and eventual decay [Fig. 4(a)] . We note that temperature-induced changes in the cavity detuning[40] or an additional delayed feedback[41] can evoke similar spontaneous symmetry breaking and motion of cavity solitons in a coherently driven optical resonator.

For an increasing pump amplitude the parametric soliton undergoes another Hopf-type bifurcation caused by a spatially symmetric eigenmode with the complex eigenvalue λ. This parametric soliton undergoes oscillations and then decays [Fig. 4(b)].

IV. EXCITATION AND DYNAMICS OF PARAMETRIC SOLITONS

To excite polariton solitons in a setting close to an experiment, one can use a seed pulse, such that an additional pump term $E_{\text{seed}}(y,t)e^{ik_{\text{seed}}x - i\Omega_{\text{seed}}t}$ is required in the original model, (1). This seed pulse has a temporal duration of several photon lifetimes and it is extended along the x and localized in the y direction. After a sufficiently long time interval (several photon lifetimes) the intracavity field evolves into a train of moving pulses [see Figs. 5(a) and 5(b)] .

Expanding these periodic solutions into Fourier series in x we find three distinct components, corresponding to the signal, idler, and pump. The y dependencies of these components coincide with the soliton profiles discussed in the previous section [see Fig. 3(c)]. The train is periodic in x with the period $P_x \approx 2\pi/|k_p - k_{\text{seed}}|$. It moves along the x direction with phase velocity $V_x \approx 2\pi|\Omega_p - \Omega_{\text{seed}}|/|k_p - k_{\text{seed}}|$. The seed pulse excites a signal polariton with the transverse momentum k_{seed} and frequency Ω_{seed} which corresponds to the effective detuning $\Delta_{\text{seed}} = \Omega_{\text{seed}} - \Omega_-(k_{\text{seed}}, k_y = 0)$ of

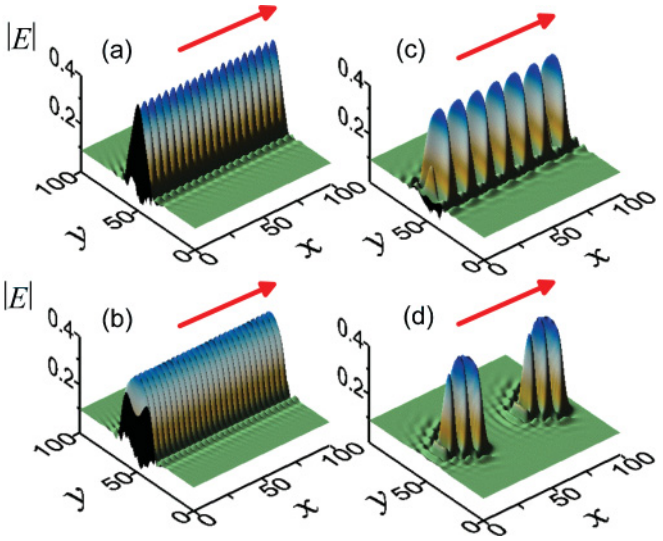

FIG. 5. (Color online) (a)-(c) 2D profiles of the parametric polariton soliton calculated in the original model, (1), for (a) $E_p = 0.136$ and $k_{\text{seed}} = 0$, (b) $E_p = 0.140$ and $k_{\text{seed}} = -0.4138$, and (c) $E_p = 0.138$ and $k_{\text{seed}} = 0.7448$. (d) Profile of a moving 2D cavity polariton soliton for $E_p = 0.1375$ and $k_{\text{seed}} = 0.4966$. The (red) arrow shows the direction of pattern motion. For all calculations, $\Omega_p = -0.25$ and the optical pump momentum is $k_p = 1.2$.

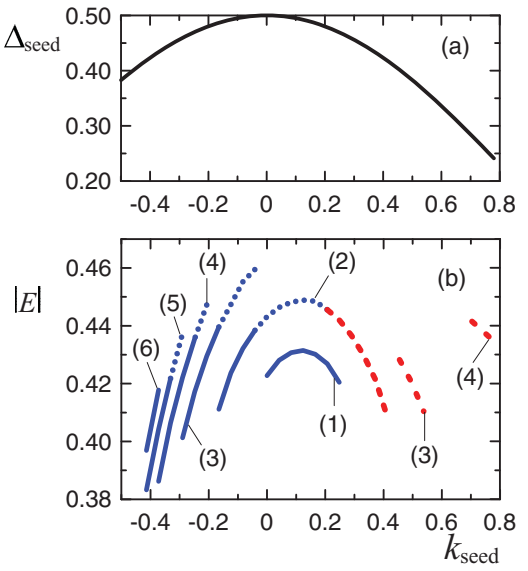

FIG. 6. (Color online) (a) Effective detuning of the signal polariton versus the seed pulse momentum ($\Omega_{\text{seed}} = -0.5$). (b) Families of parametric polariton solitons as a function of the seed pulse momentum (k_{seed}) calculated in the original model, (1), for different amplitudes of the pump beam: (1) $E_p = 0.1355$, (2) $E_p = 0.136$, (3) $E_p = 0.137$, (4) $E_p = 0.138$, (5) $E_p = 0.139$, and (6) $E_p = 0.140$. For all calculations, $\Omega_p = -0.25$ and the optical pump momentum is $k_p = 1.2$.

the model considered in the previous section [see Fig. 6(a)]. The amplitude and period of the pattern depend on the transverse momentum of the seed pulse k_{seed}. Figure 6(b) gives a summary of the families of parametric polariton solitons for different pump amplitudes and k_{seed} values (for a fixed seed power and the frequency $\Omega_{\text{seed}} = -0.5$). We note that only stable (dynamically) and slightly unstable solutions can be obtained solving the dynamical model, (1). As shown in the previous section [Fig. 2(a)], the existence domain of a stable parametric polariton soliton shifts into the direction of lower optical pump amplitudes (E_p) for increasing signal detunings (Δ_s). In qualitative agreement, the seed pulse with the low momentum $k_{\text{seed}} \approx 0$ [and thus with the maximum detuning; see Fig. 6(a)] excites a parametric polariton soliton for a weaker optical pump E_p (and vice versa). The slight asymmetry with respect to $k_{\text{seed}} = 0$ can be explained by the fact that the effective masses of the signal and the idler polaritons are not constants as assumed in the model, (5)–(7). Our results unambiguously show the existence of a soliton family which is continuously parameterized by the transverse momentum of the signal beam. Choosing an appropriate seed momentum we can excite parametric solitons almost in the entire interval where the pump-only HS is bistable.

There is a qualitative difference in the stability properties of parametric polariton solitons for negative and positive values of k_{seed}. Decreasing the momentum offset between the signal and the pump polaritons ($k_p - k_{\text{seed}}$) usually results in soliton destabilization on time scales much larger than the polariton lifetime (see dotted and dashed lines in Fig. 6(b)]. For negative momenta k_{seed} the solitons found by direct numerical modeling of Eqs. (1) inherit both destabilization scenarios discussed in the previous section. Indeed, the parametric polariton solitons undergo both symmetry breaking and motion instability [similar to Fig. 4(a)] or they become oscillatory unstable [similar to Fig. 4(b)], while increasing either the pump amplitude or the signal momentum [see dotted lines in Fig. 6(b)].

For positive k_{seed}, the parametric polariton soliton can become modulationally unstable against periodically modulated perturbations in the x direction, i.e., along the direction of the pump momentum [see dashed (red) lines in Fig. 6(b)]. This modulational instability can trigger the fragmentation of the periodic pattern into a train of well-separated 2D structures [see Fig. 5(c)], which have a straightforward association with the 2D solitons reported in our recent work.[28] Other types of periodic trains of well-isolated multipeak structures have also been observed in our modeling; see an example of the triple-peak structures in Fig. 5(d).

V. SUMMARY AND DISCUSSION

The above results demonstrate that four-wave mixing of microcavity polaritons promotes their localization in the direction associated with the positive effective mass. As a result, stable bright parametric solitons can be formed in the direction orthogonal to the pump momentum. Unlike nonparametric cavity solitons,[39] they constitute a one-parameter soliton family. This soliton family can be continuously parameterized with the transverse momentum of the signal polariton, whereas the phase matching condition fixes the momentum of the idler component. The frequency matching conditions together with the energy balance between signal and idler polaritons provide strict selection rules for the frequencies of the signal and idler

components of the parametric polartion soliton. Any solution of this soliton family can be excited by means of a seed pulse with the appropriate momentum and frequency. Modulational instability can trigger the parametric polariton soliton into a train of well-separated 2D polariton solitons reported in our recent work.[28]

Apart from the fundamental significance of our findings, they hold promise for practical applications. This promise arises from the fast and strong nonlinear response of exciton-polaritons,[5] prevailing in these aspects against the pure optical nonlinearity in semiconductor microcavities in the weak-coupling regime, where very attractive applications of 2D cavity solitons[39] have suffered from the slow excitation times and high power requirements.

ACKNOWLEDGMENTS

Financial support by the Federal Ministry of Education and Research (PhoNa) and the Deutsche Forschungsgemeinschaft (Research Unit 532) is acknowledged.

*Corresponding author: oleg.egorov@uni-jena.de

[1] C. Weisbuch, M. Nishioka, A. Ishikawa, and Y. Arakawa, Phys. Rev. Lett. **69**, 3314 (1992).
[2] R. Houdre, R. P. Stanley, U. Oesterle, M. Ilegems, and C. Weisbuch, Phys. Rev. B **49**, 16761 (1994).
[3] H. Haug and S. W. Koch, *Quantum Theory of the Optical and Electronic Properties of Semiconductors*, 2nd ed. (World Scientific, Hong Kong, 1993).
[4] B. Deveaud, *The Physics of Semiconductor Microcavities* (Wiley-VCH, New York, 2007).
[5] A. Kavokin, J. Baumberg, G. Malpuech, and F. Laussy, *Microcavities* (Oxford University Press, New York, 2007).
[6] S. Schmitt-Rink, D. S. Chemla, and D. A. B. Miller, Phys. Rev. B **32**, 6601 (1985).
[7] G. Rochat, C. Ciuti, V. Savona, C. Piermarocchi, A. Quattropani, and P. Schwendimann, Phys. Rev. B **61**, 13856 (2000).
[8] J. Kasprzak, M. Richard, S. Kundermann, A. Baas, P. Jeambrun, J. M. Keeling, F. M. Marchetti, M. H. Szymanska, R. Andre, J. L. Staehli, V. Savona, P. B. Littlewood, B. Deveaud, and L. S. Dang, Nature **443**, 409 (2006).
[9] R. Balili, V. Hartwell, D. Snoke, L. Pfeiffer, and K. West, Science **316**, 1007 (2007).
[10] D. Sanvitto, A. Amo, F. P. Laussy, A. Lemaitre, J. Bloch, C. Tejedor, and L. Vina, Nanotechnology **21**, 134025 (2010).
[11] I. Carusotto and C. Ciuti, Phys. Rev. Lett. **93**, 166401 (2004).
[12] A. Amo, J. Lefrere, S. Pigeon, C. Adrados, C. Ciuti, I. Carusotto, R. Houdre, E. Giacobino, and A. Bramati, Nature Phys. **5**, 805 (2009).
[13] A. Amo, D. Sanvitto, F. P. Laussy, D. Ballarini, E. del Valle, M. D. Martin, A. Lemaitre, J. Bloch, D. N. Krizhanovskii, M. S. Skolnick, C. Tejedor, and L. Vina, Nature **457**, 291 (2009).
[14] A. Amo, D. Sanvitto, and L. Vina, Semicond. Sci. Technol. **25**, 43001 (2010).
[15] S. Christopoulos, G. Baldassari Höger von Högersthal, A. J. D. Grundy, P. G. Lagoudakis, A. V. Kavokin, J. J. Baumberg, G. Christmann, R. Butte, E. Feltin, J.-F. Carlin, and N. Grandjean, Phys. Rev. Lett. **98**, 126405 (2007).
[16] A. Tredicucci, Y. Chen, V. Pellegrini, M. Börger, and F. Bassani, Phys. Rev. A **54**, 3493 (1996).
[17] A. Baas, J. P. Karr, H. Eleuch, and E. Giacobino, Phys. Rev. A **69**, 023809 (2004).
[18] D. Bajoni, E. Semenova, A. Lemaitre, S. Bouchoule, E. Wertz, P. Senellart, S. Barbay, R. Kuszelewicz, and J. Bloch, Phys. Rev. Lett. **101**, 266402 (2008).
[19] A. Baas, J. P. Karr, M. Romanelli, A. Bramati, and E. Giacobino, Phys. Rev. B **70**, 161307(R) (2004).
[20] C. Ciuti, P. Schwendimann, B. Deveaud, and A. Quattropani, Phys. Rev. B **62**, 4825(R) (2000).
[21] C. Ciuti, P. Schwendimann, and A. Quattropani, Semicond. Sci. Technol. **18**, 279 (2003).
[22] D. M. Whittaker, Phys. Rev. B **63**, 193305 (2001).
[23] P. G. Savvidis, J. J. Baumberg, R. M. Stevenson, M. S. Skolnick, D. M. Whittaker, and J. S. Roberts, Phys. Rev. Lett. **84**, 1547 (2000).
[24] D. M. Whittaker, Phys. Rev. B **71**, 115301 (2005).
[25] M. Wouters and I. Carusotto, Phys. Rev. B **75**, 075332 (2007).
[26] O. A. Egorov, D. V. Skryabin, A. V. Yulin, and F. Lederer, Phys. Rev. Lett. **102**, 153904 (2009).
[27] D. V. Skryabin, O. A. Egorov, A. V. Gorbach, and F. Lederer, Superlattices Microstruct. **47**, 5 (2010).
[28] O. A. Egorov, A. V. Gorbach, F. Lederer, and D. V. Skryabin, Phys. Rev. Lett. **105**, 073903 (2010).
[29] A. V. Buryak, P. Di Trapani, D. V. Skryabin, and S. Trillo, Phys. Rep. **370**, 63 (2002).
[30] D. V. Skryabin, Phys. Rev. E **60**, 3508(R) (1999).
[31] D. V. Skryabin, A. R. Champneys, and W. J. Firth, Phys. Rev. Lett. **84**, 463 (2000).
[32] C. Etrich, D. Michaelis, and F. Lederer, J. Opt. Soc. Am. B **19**, 792 (2002).
[33] D. Michaelis, U. Peschel, C. Etrich, and F. Lederer, IEEE J. Quant. Electron. **39**, 255 (2003).
[34] P. Di Trapani, G. Valiulis, A. Piskarskas, O. Jedrkiewicz, J. Trull, C. Conti, and S. Trillo, Phys. Rev. Lett. **91**, 93904 (2003).
[35] A. V. Yulin, O. A. Egorov, F. Lederer, and D. V. Skryabin, Phys. Rev. A **78**, 061801(R) (2008).
[36] J. J. Hopfield, Phys. Rev. **112**, 1555 (1958).
[37] D. Avitabile, D. J. B. Lloyd, J. Burke, E. Knobloch, and B. Sandstede, SIAM J. Appl. Dyn. Syst. **9**, 704 (2010).
[38] N. Akhmediev and A. Ankiewicz, *Dissipative Solitons* (Springer, Berlin, 2005).
[39] T. Ackemann, W. J. Firth, and G. Oppo, Adv. At. Mol. Opt. Phys. **57**, 323 (2009).
[40] A. J. Scroggie, J. M. McSloy, and W. J. Firth, Phys. Rev. E **66**, 036607 (2002).
[41] M. Tlidi, A. G. Vladimirov, D. Pieroux, and D. Turaev, Phys. Rev. Lett. **103**, 103904 (2009).